energy&fuels

pubs.acs.org/EF

Article

Gas-Phase Potassium Effects and the Role of the Support on the Tar Reforming of Biomass-Derived Producer Gas Over Sulfur-Equilibrated Ni/$MgAl_2O_4$

Asbel Hernandez, Klas J. Andersson, Klas Engvall,* and Efthymios Kantarelis

Cite This: *Energy Fuels* 2020, 34, 11103−11111

Read Online

ACCESS | Metrics & More | Article Recommendations

ABSTRACT: Biomass gasification is a sustainable way to convert biomass residues into valuable fuels and chemicals via syngas production. However, several gas impurities need to be removed before the final synthesis. Understanding of the interactions and effects of biomass-derived producer gas contaminants (S and K) on the performance of reforming catalysts is of great importance when it comes to process reliability and development. In the present study, the steam reforming activity at 800 °C of a sulfur-equilibrated nickel catalyst during controlled exposure to alkali species (~2 ppmv K) and in its absence was investigated using real producer gas from a 5 kW_{th} O_2-blown fluidized-bed gasifier. Conversions of CH_4, C_2H_4, and $C_{10}H_8$ were used to evaluate the performance of the Ni/$MgAl_2O_4$ catalyst and $MgAl_2O_4$ support. A significant and positive effect on the catalyst activity is observed with addition of gas-phase KCl. This is assigned primarily to the observed K-induced reduction in sulfur coverage (θ_S) on Ni—an effect which is reversible. The catalytic contribution of the K-modified pure $MgAl_2O_4$ support was found to be significant in the conversion of naphthalene but not for light hydrocarbons. The product and catalyst analyses provided evidence to elucidate the preferential adsorption site for S and K on the catalyst as well as the role of the support. Whereas S, as expected, was found to preferentially adsorb on the surface of Ni particles, forming S-Ni sites, K was found to preferentially adsorb on the $MgAl_2O_4$ support. A low but still significant K adsorption on S−Ni sites, or an effect on only the fraction of exposed Ni surface area near the metal−support interface, can, however, not be excluded. The result suggests that an improved Ni/$MgAl_2O_4$ catalyst activity and an essentially carbon-free operation can be achieved in the presence of controlled amount of gas-phase potassium and high sulfur coverages on Ni. Based on the results, a mechanism of the possible K−S interactions is proposed.

INTRODUCTION

Biomass is regarded as a renewable resource suitable for addressing our increasing energy needs and simultaneously contributing toward a more sustainable society.[1] An attractive solution for an efficient conversion of a wide range of biomass feedstock to useful energy carriers, for further upgrading to valuable products, is gasification.[2−4]

Producer gas derived from biomass gasification units contains considerable amounts of secondary products, such as light and heavy organic compounds,[5] and different levels of particulates and inorganic impurities,[6−8] depending on the type of gasifier and biomass feedstock.

According to Milne et al.,[5] tar levels, i.e., (poly)aromatic hydrocarbons, are in the range of 1−100 g/(N m^3), where in general terms, downdraft gasifiers are considered as the cleanest; updraft gasifiers have the highest levels and fluidized-bed (FB) gasifiers are in the lower intermediate range.[5] A high content of such impurities can be problematic from an operating point of view with condensation, plugging, and corrosion, being encountered inside and/or downstream the gasifiers. Additionally, formation of carbon deposits due to high tar content on catalysts in downstream processes[9,10] constitutes a large problem. Therefore, the challenge is to remove or convert these problematic organic compounds into useful syngas molecules.[10] An attractive method to do so is secondary catalytic tar reforming, converting tar into permanent gases.[2] Catalytic tar reforming has been performed with numerous types of Ni-based and noble-metal catalysts.[6,10−14] Ni-based catalysts are nevertheless considered as the most cost-effective for tar reforming applications.[12,15]

However, catalysts for tar reforming are exposed to several impurities and contaminants, such as particulates and inorganic trace compounds (alkali, sulfur, nitrogen, and chlorine species) present in the producer gas.[6−8,16] The concentration of these components depends on several parameters, such as gasification technology used, process conditions, type of biomass, and choice of technology for gas cleaning upstream of the catalytic reactor. Typical gas-phase K-species levels are around 0.01−5 ppmv (db),[7,17,18] with one case reported as high as 54 ppmv (db).[8] The concentration of particulates in the gas ranges between 5 and 30 g/(N m^3),[19] consisting of unconverted biomass material in the form of ash, char, and bed material in the case of fluidized-bed gasification. As far as S

Received: June 22, 2020
Revised: August 12, 2020
Published: August 17, 2020

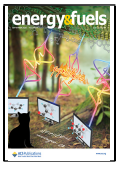

(mainly H_2S and some COS) and Cl (mainly HCl) compounds are concerned, their levels in the biomass producer gas are generally 20−200 ppmv (db),[6] while typical NH_3 concentration is in the range of 500−3000 ppmv (db) when woody biomass is used.[20]

Cl and NH_3 at the concentrations discussed do not affect the reforming performance of the Ni catalysts,[21,22] but sulfur and alkali compounds play an important role in the activity of tar reforming Ni-based catalysts. Contradictory effects for the presence of K and S have been reported in the literature. Investigations[23,24] on K-promoted Ni catalysts report on minimization of carbon formation, while, on the other hand, K concentrations above a certain threshold are responsible for reduction in steam reforming[24,25] and hydrogenation activity.[26] In addition, even though S is a known and severe poison for Ni-based steam reforming catalysts, it also tends to inhibit the formation of whisker carbon above certain surface coverages, due to blockage of C nucleation sites.[24,25,27,28] Ideally, tar reforming catalysts in biomass-derived producer gas environment would have just enough S and K additives to inhibit coke formation but still maintain an appreciable reforming activity.[28]

Studies examining the effect of gas-phase alkali present in the producer gas on tar reforming catalysts are limited.[29−32] In all of these studies, the method used to investigate the influence of K on catalyst differs significantly from actual mechanisms of K transport, deposition, and equilibration on the catalyst surface.[31] A few of these studies were performed under exposure to a real producer gas from biomass and none were investigated under realistic steady-state conditions.[29−31,33] The general observation is a general decrease of the reforming activity and a loss in the surface area of Ni. Nevertheless, none of the studies offered a clear picture of the combined effects of S and K on Ni-based catalysts under steady-state conditions.

In our previous studies, we first developed and implemented a methodology enabling controlled investigation of the influence of gas-phase alkali on a tar reforming $Ni/MgAl_2O_4$ catalyst activity under realistic steady-state conditions by eliminating transient effects, caused by sulfur poisoning and sintering and by tailoring the S surface coverage by adjusting the H_2S/H_2 ratio.[34] The methodology was further applied in a study investigating the combined effects of biomass-derived gas-phase potassium at varying concentrations together with sulfur on tar reforming catalyst performance.[35] In summary, these studies provided information concerning the equilibrium K coverage on a typical Ni-based steam reforming catalyst under tar reforming conditions. A significant finding was the actual increase in the catalyst activity toward methane and tar reforming, as the K surface content increased, contradictory to previous studies.[29−31] This indicates interactions of K with S at the active Ni sites and/or support and a subsequent decrease in sulfur content on the catalyst surface with increasing K coverage. It was also suggested that the significantly increased reactivity toward tar molecules could partly be due to a K-modified support surface.

Although a step forward, extended methane and tar reforming activity studies during the K desorption phase are needed to gain further insight into the importance of the K-modified support surface reactivity and preferential sites of adsorption for S and K.

In the present study, we aim at shedding light upon the role of the support, S and K interactions with the support, and the latter's contribution to the overall catalytic activity, including an investigation on the preferential site of adsorption site (support and Ni metal) of the K and S species on a Ni catalyst.

The individual roles of Ni and support are elucidated during separate K desorption from the $Ni/MgAl_2O_4$ catalyst and pure $MgAl_2O_4$ support under steam reforming conditions, and an overall mechanism is proposed. The above effects are of great importance when considering gas conditioning requirements and energy efficiency, especially for applications like dusty gas autothermal reforming and/or development of catalytic particulate filters.

MATERIALS AND METHODS

Materials. Pine pellets of 1.5−2 mm were used as biomass feedstock, and their ultimate and proximate analysis results are shown in Table 1.

Table 1. Proximate and Ultimate Analyses of Biomass Used[a]

proximate analysis	
moisture (wt %)	7.40
ash (wt % db)	0.52
volatile matter (wt % db)	80.1
fixed carbon (wt % db)	19.4
ultimate analysis	
C (wt % db)	47.7
H (wt % db)	6.3
N (wt % db)	0.16
S (wt % db)	<0.012
O (wt % db)	45.3
Cl (wt % db)	0.03
K (mg/kg db)	639
Cl (mg/kg db)	57.3

[a]db: dry basis.

The biomass was chosen due to its low ash content, minimizing biomass ash-derived effects on tar reforming. Nonporous alumina with a particle size of 63−125 μm was used as a bed material in the gasifier. The $Ni/MgAl_2O_4$ catalyst and the $MgAl_2O_4$ support are aged and surface-saturated with S and K under controlled conditions at the same time with real biomass-derived producer gas with simultaneous monitoring of tar and methane reforming activity. The Ni-based catalyst $Ni/MgAl_2O_4$ and magnesium aluminate ($MgAl_2O_4$-spinel) support were provided in a pellet form by Haldor Topsoe (Haldor Topsoe A/S HT-25934 and HT-80541, respectively). Prior to use, both the catalyst and the support were ground to an average particle size of 3.6 mm (3.15 < dp < 4.0 mm). Inert nonporous silica-free fillers (Vereinigte Füllkörper-Fabriken, Duranit Inert D99) of 3.175 mm diameter were used as bed diluent.

Methods. For the experimental investigation, a 5 kW_{th} bubbling fluidized-bed (FB) gasifier coupled to a particulate filter and a fixed-bed catalytic reactor was used. An alkali aerosol generator with a diffusion dryer was connected at the outlet of the particulate filter. More details about the experimental setup and alkali dosing system can be found elsewhere.[34]

The experimental procedure consisted of three stages, namely, (i) catalyst aging and pretreatment; (ii) gasification and tar reforming with alkali dosing (surface saturation stage); and (iii) continued gasification and tar reforming without alkali addition (K-decay stage).

Prior to pretreatment of the catalyst and support, the experimental setup was cleaned by steaming at 900 °C for 12 h to volatilize any residual K located on the walls of the system upstream the reformer and thus minimize the risk of K uptake other than from the alkali aerosol generator. Initially, 25 g of catalyst and 25 g of support were mixed with 50 g of inert diluent and subjected to activation by reduction in H_2 at 550 ± 1 °C for 5 h. After reduction, the bed was

https://dx.doi.org/10.1021/acs.energyfuels.0c02069
Energy Fuels 2020, 34, 11103−11111

subjected to steam aging at 900 °C for 5 h at a steam/H_2 molar ratio of 10.

Aging with steam stabilizes the catalyst and minimizes any further sintering that would result in erroneous interpretation of activity changes during operation. To eliminate any transient phenomena due to a gradual S-coverage of the catalyst during operation, the catalyst and the support were subjected to "sulfidation" at 803 ± 2 °C at a H_2S/H_2 ratio of 1.88×10^{-4} for 4 h (bulk sulfide (Ni_3S_2) is expected to form at ratios greater than 0.001[36]). The H_2S/H_2 ratio has been determined experimentally and is the resultant ratio during gasification of biomass under the experimental conditions used in the study. The actual sulfur coverage, θ_S, at this temperature and sulfidation conditions (H_2S/H_2) would yield a sulfur coverage of ~0.96 according to Alstrup et al.[37] The coverage (θ) as a function of temperature for different H_2S/H_2 ratios is depicted in Figure 1.

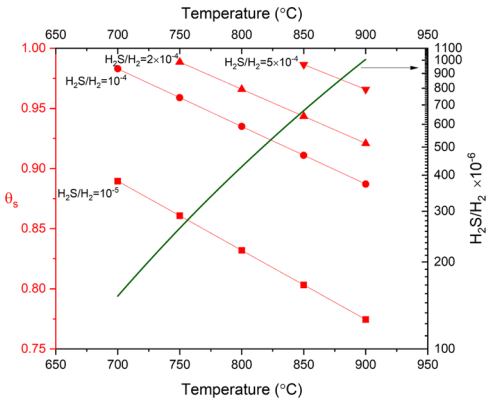

Figure 1. Ni sulfur coverage (θ_S) as a function of temperature and H_2S/H_2 ratio. The solid line corresponds to θ_S = 1 at different temperatures.

Once the catalyst and the support were "sulfided," they were directly exposed to producer gas from the gasifier with additional KCl from the aerosol generator until saturation of the surface (surface saturation stage). The duration of saturation stage was determined based on previous results performed under similar conditions (catalyst saturation of K uptake of the catalysts was achieved in ~20 h on stream[35]). The completion of saturation stage was also verified by the observed stable conversion of CH_4, C_2H_4, and $C_{10}H_8$. After the saturation stage, the bed was removed, and the catalyst and support were separated. The catalyst and the bed diluent were then mixed with additional inert diluent occupying the same volume as the support to ensure similar hydrodynamic behavior of the catalyst bed between the saturation and decay stages. The catalyst bed was then placed in the reactor and exposed to the producer gas but without KCl aerosol (decay stage). Identical space velocities between saturation and decay stages were achieved by substituting the aqueous KCl solution in the aerosol generator with Millipore water. The duration of the catalyst activity decay stage was again determined by the observed conversion of methane and naphthalene ($C_{10}H_8$). The same procedure was followed for the support as well.

Differences in conversion due to the absence of the support in the initial and final stages of K-decay period would provide information about the presence of K and the role of the support during the tar conversion. To address the thermal effects in the absence of potassium, the bed in the catalytic reactor was replaced by inert diluent occupying the same volume as the catalyst and the support. Gas-phase reactions affected by the addition of KCl aerosol to the system[38] were assessed by injecting the aerosol and using an empty reactor. The detailed experimental conditions are shown in Table 2.

Dry gas composition was determined using a Thermo Scientific C2V-200 micro-GC, while the tar content in the gas was determined by the solid-phase adsorption (SPA) method.[39]

The catalyst and the support were characterized by means of N_2 physisorption using an ASAP 2010 instrument for Brunauer–Emmett–Teller (BET) surface area determination and by ICP/MS for S and K content determination. Carbon content was determined using a LECO CS230 analyzer. Upon completion of each of the experimental stages, a small amount of catalyst and/or support was withdrawn for characterization. More details about the sampling procedure are provided elsewhere.[34,35]

Table 2. Experimental Conditions Used in This Study

gasification agent	O_2
biomass feeding rate (g/h)	208 ± 2
λ	0.24–0.25
average bed temperature (°C)	820 ± 6
average freeboard temperature (°C)	733 ± 5
filter temperature (°C)	850 ± 2
reformer temperature (°C)	803 ± 3
GHSV (h^{-1})	11 617 ± 981[a]

[a]At 803 °C, excluding N_2, and in all cases reported herein with a fixed total bed volume (catalyst + support + inert diluent) of 97 mL.

The catalytic activity was evaluated by continuous monitoring of methane, ethylene, and naphthalene conversions. The conversion was calculated according to eq 1

$$X_i = 1 - \frac{F_{i,\text{out}}}{F_{i,\text{in}}} \quad (1)$$

where X_i, $F_{i,\text{out}}$, and $F_{i,\text{in}}$ are the conversion and the molar flow at the outlet and inlet of species i (mol/h), respectively. The estimated error (standard deviation) in the computed variables (e.g., X_i) from the experimental data has been determined as follows[39]

$$z \pm Dz = f(a \pm Da,\ b \pm Db,\ \ldots,\ n \pm Dn) \quad (2)$$

where z is the computed variable from experimental datasets (a, b, ..., n), f is a function that corresponds to the mathematical operation (addition/subtraction or division/multiplication), and Dz, Da, Db, ..., Dn are the corresponding standard deviations of the computed variable(z) and the corresponding average values of measured data (a, b, ..., n).

For addition/subtraction operations, the standard deviation of the computed variable was calculated according to

$$Dz = \sqrt{(Da)^2 + (Db)^2 + \ldots + (Dn)^2} \quad (3)$$

While for division and multiplication, the computed error was determined as follows

$$\frac{Dz}{z} = \sqrt{\left(\frac{Da}{a}\right)^2 + \left(\frac{Db}{b}\right)^2 + \ldots + \left(\frac{Dn}{n}\right)^2} \quad (4)$$

RESULTS AND DISCUSSION

The producer gas composition was stable throughout the tests and the average composition of N_2-free gas as well as gas and tar flows to the catalytic steam reformer are listed in Table 3. It has to be noted that the time on stream corresponds to cumulative experimental time and average gas composition refers to time-weighted average of the different gasification runs under the experimental conditions listed in Table 2. The water content in the gas has been determined based on the water gas shift reaction equilibrium.[40,41]

The Ni catalyst suffered an initial loss in surface area, due to the accelerated aging step, but no further surface area loss is observed (Figure 2). Contrary to the Ni catalyst, the $MgAl_2O_4$ support maintained its surface area throughout the aging and testing stages. This comes as no surprise because the $MgAl_2O_4$ support system was calcined in air at several hundred degrees above 900 °C before Ni was added to the system. Hence, the

https://dx.doi.org/10.1021/acs.energyfuels.0c02069
Energy Fuels 2020, 34, 11103–11111

Table 3. Average Composition of Producer Gas (N_2-Free) at the Inlet of the Catalytic Reactor

Nm^3 gas/$kg_{biomass}$	1.42 ± 0.02
compound	(% mol)
CO_2	19.95 ± 0.05
C_2H_4	1.65 ± 0.01
CH_4	7.19 ± 0.01
CO	27.52 ± 0.11
H_2	25.25 ± 0.15
H_2O	17.86 ± 0.11
tar excluding benzene (g/h)	8.7 ± 1.1
$C_{10}H_8$ (g/h)	6.2 ± 0.9
C_{10+} (g/h)	1.6 ± 0.6
KCl (from biomass)	<0.2 ppmv[35]
KCl (from aerosol)	1.8 ppmv
H_2S	15 ± 3 ppmv

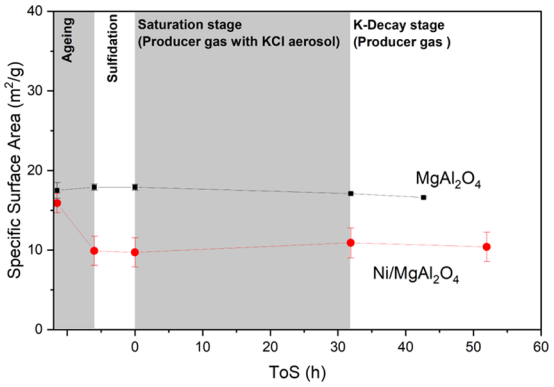

Figure 2. Effect of thermal aging and changes in surface area of catalyst and support during the different stages of treatment and catalytic runs (0 time on stream refers to the moment that the catalyst and the support are exposed to producer gas from the gasifier).

loss in surface area for the $Ni/MgAl_2O_4$ catalyst due to the 900 °C H_2O/H_2 aging procedure is therefore explained solely by the loss of Ni surface area, i.e., the sintering of the metallic Ni particles. Therefore, the catalyst reaches a stable performance and Ni sintering should not be considered to have an important role in any activity changes. The BET surface areas for the carrier, fresh catalyst, and aged catalysts are all in the range of 10−20 m^2/g, similar to the areas reported in previous work.[34] Earlier studies indicated that K deposition can accelerate sintering of Ni particles under certain conditions.[25] However, as is already obvious from Figure 2, in our case, alkali dosing does not affect the total surface area of the catalyst once thermally stabilized and does not affect the specific Ni surface area as judged by the very similar S content before K-dosing and after significant K removal in the decay stage. These findings also rule out any significant Cl-induced Ni sintering[42] in the present study. Unaffected specific surface area upon deposition of K and relatively constant pore volume, which lies in the range of 100−150 mL/kg for fresh, aged, and spent materials, also indicate that the deposition was done from gas-phase species and that no molten KCl was deposited on the surface blocking the pores, as reported elsewhere.[33] This suggests that the real mechanism of K deposition on the surface is different from the impregnation studies.[29−31,33]

In Figure 3, changes in sulfur and potassium surface coverages, during saturation and decay stages, are shown, which are indicative of adsorption−desorption reversibility.

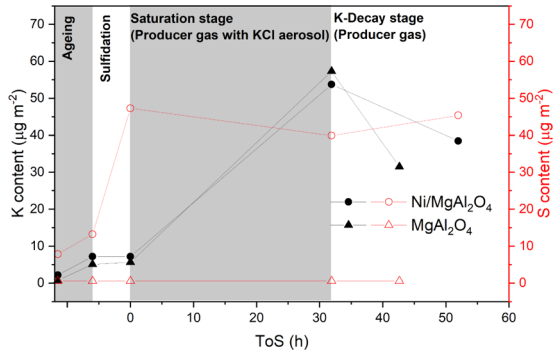

Figure 3. Surface area normalized K and S uptakes of catalyst and support during different phases of treatment and catalytic runs (0 h on stream refers to the moment that the catalyst and the support are exposed to producer gas from the gasifier) (combined standard deviations are insignificant and are not shown in the figure).

The findings corroborates our previous results,[35] observing a significant decrease in the sulfur content of the $Ni/MgAl_2O_4$ system upon K-saturation/equilibration, increasing again at the end of the K-decay period.

Sulfur sorption takes place only on $Ni/MgAl_2O_4$ (Figure 3), proving the clear preferential adsorption of S on Ni sites compared to the $MgAl_2O_4$ support. Hence, it can be postulated that any potential K−S interaction occurs on the Ni sites or in the proximity of the Ni sites, while spillover of S from the Ni sites to the support is very small, if at all relevant.

The K surface concentration in Figure 3 at K-equilibration is very similar on the carrier ($MgAl_2O_4$) and on the catalyst ($Ni/MgAl_2O_4$), ca. 55 $\mu g\ K/m^2$ BET (0.67 K/nm^2 BET) in both cases. This is slightly higher than the 10−40 $\mu g\ K/m^2$ BET in our previous work,[35] but still well below the extrapolated maximum of 100 $\mu g\ K/m^2$ BET therein. Given that the K surface concentration is very similar for the catalyst and the pure carrier, if K is present on S−Ni sites, it is so in much lower total amounts than K on the carrier (ca. 0.67 K/nm^2 BET), and the adsorbed sulfur amount on Ni, ca. 40 $\mu g\ S/m^2$ BET (0.59 S/nm^2 BET). Based on our results here, potassium species can be located: (a) on the support, clearly providing the main fraction of K adsorption sites, relatively far from the active nickel sites; (b) in close proximity to the active nickel sites, e.g., Ni-support interface forming K−O−Ni complexes;[43] and (c) on S−Ni sites, but only to a small extent. The absence of S at the surface (S_{ads}) of the K-saturated $MgAl_2O_4$ infers that any direct interaction of gaseous H_2S with support-sorbed potassium (K_{ads}) or interaction of S_{ads} and K_{ads} in the close vicinity of the Ni sites would result in a desorbed product. With respect to K adsorption on the S−Ni system, it has previously been shown to preferentially take place on top of the more strongly bound surface sulfur (S−Ni) on Ni(100).[44] In the same study, KS desorption products from Ni(100) were reported for sulfur coverages above S−Ni monolayer saturation (S/Ni > 0.5, $\theta_S > 1$). However, gaseous K−S compounds were not measured in our experiments, and gas-phase thermodynamic equilibrium calculations, carried out in the present study, show that KS concentrations should be negligible, compared to H_2S. K−S compounds can therefore not be an important S sink under our experimental conditions.

The origin of the ∼10% lower S-coverage on Ni upon K coadsorption during tar reforming conditions remains unsolved despite our additional studies here, including also the $MgAl_2O_4$ carrier. Potassium catalyst modification is known

https://dx.doi.org/10.1021/acs.energyfuels.0c02069
Energy Fuels 2020, 34, 11103−11111

to increase the rate of water splitting.[45,46] Thus, faster O(H) transport to Ni may take place that could inhibit the S adsorption or affect S sorption/desorption rates, particularly at the gas-phase exposed Ni surface sites located at, and very near, the Ni/$MgAl_2O_4$ interface. The effective local concentration of K is also very high in this metal−support interface region, where K adsorption and chemical bonding at S−Ni sites[47−49] may induce a significant S−Ni bond weakening per adsorbed K, leading to a reduced equilibrium S-coverage, as previously discussed.[35] The effect of K on sulfur vacancies and defects in the S−Ni overlayer could be extended (nonlocal) in a way similar to Cs adsorbed on the O−Cu system.[50] Whether a result of higher O(H) surface concentrations or the adsorbed K, or both, the ∼10% lower θ_S on Ni, in the presence of 2 ppmv K in the gas phase, very likely primarily reflects the local changes in S-coverage on Ni sites near the metal−support interface. The increase in S-free Ni sites leads to drastically increased methane and ethylene conversions as observed and naturally leads to higher probabilities of larger S-free Ni site ensembles better able to steam-reform larger hydrocarbons such as naphthalene.

The effects of potassium adsorption and desorption on the reforming activity of CH_4, C_2H_4, and $C_{10}H_8$ are shown in Figures 4−6, respectively. For all of the compounds monitored,

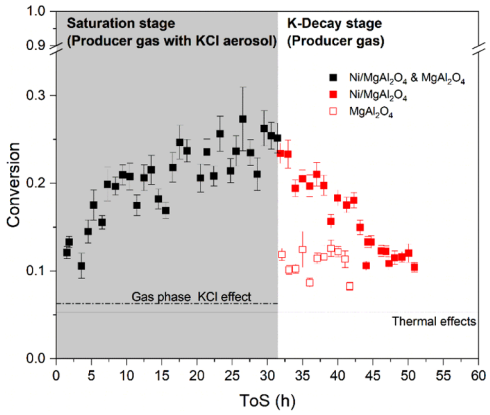

Figure 4. Average CH_4 conversion versus time on stream.

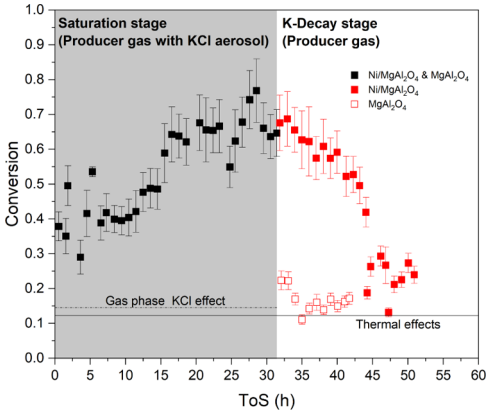

Figure 5. Average C_2H_4 conversion versus time on stream.

the thermal effects (solid horizontal line) have only a rather small impact on their conversion. Thermal effects are becoming more important in the following order CH_4 < C_2H_4 < $C_{10}H_8$, following the compounds' respective thermal

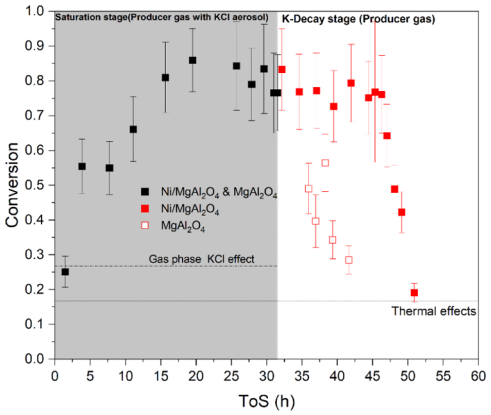

Figure 6. Average $C_{10}H_8$ conversion versus time on stream.

stability.[51] Introduction of gas-phase potassium has an effect on the gas-phase conversion of hydrocarbons, as also reported elsewhere;[52] however, this effect is limited (dash-dotted horizontal line) and is more pronounced for the bulkier tar molecules.[38] The initial conversion observed for all hydrocarbons corresponds to the conversion achieved with $\theta_S \sim 0.96$ on Ni given that potassium equilibration is first achieved after more than 10 h on stream. As expected,[53] the initial catalytic activity is low for such a high S-coverage on Ni and low operating temperature.

Introduction of potassium results in a gradual and, over time, drastic steam reforming activity increase for all of the hydrocarbons in question. A stable conversion is achieved after approximately 15 h for methane and ethylene and after 20 h for naphthalene. The stable conversion indicates that potassium is in equilibrium with the catalyst surfaces at stable adsorption−desorption rates.

The conversions of CH_4 and C_2H_4 during the K-saturation stage are illustrated in Figures 4 and5, respectively. As shown, the conversion of C_2H_4 displayed similar trends to CH_4, although C_2H_4 conversion values obtained were higher. This is so despite the fact that formation of C_2H_4 caused by gas-phase reactions of tar compounds during KCl dosing could be expected due to the promoted cracking and dehydrogenating effect of K under tar reforming conditions.[38,54]

Figure 6 depicts the conversion of $C_{10}H_8$. The total error of each point is considerably higher than that in the case of the lighter hydrocarbons due to the greater error sources and uncertainties during the sampling, extraction, identification, and quantification steps, associated with the SPA method.[55] Nevertheless, a strong positive effect on the $C_{10}H_8$ conversion during the K-saturation phase is observed.

As seen in Figures 4−6, the falloff values in conversion during the K-decay phase over the Ni/$MgAl_2O_4$ catalyst are quite different for CH_4 and C_2H_4 compared to $C_{10}H_8$. This could be related to the different reactivities of the molecules, differences in internal mass transfer limitations between the molecules,[34] the way the intrinsic activity toward the different molecules changes on a local scale inside the catalyst particles because of the K concentration profile dynamically changing inside the catalyst particles and throughout the bed during the K-decay stage, and the fact that the K-doped $MgAl_2O_4$ support is active toward naphthalene and not CH_4 and C_2H_4, as will be discussed later. The calculated effective diffusivities (D_{eff})[56−59] for CH_4, C_2H_4, and $C_{10}H_8$ are equal to 4.83×10^{-7}, 3.65×10^{-7}, and 1.71×10^{-7} m^2/s, respectively, under the

https://dx.doi.org/10.1021/acs.energyfuels.0c02069
Energy Fuels 2020, 34, 11103−11111

experimental conditions of the study, indicating the slower diffusion of larger tar molecules in the catalyst particles. The lower the D_{eff}, the more sensitive the conversion rate becomes to the conditions at the outermost volume of the catalyst particles. The significantly later falloff in naphthalene conversion, compared to CH_4 and C_2H_4, could suggest initially higher K concentrations in the outermost volume of the catalyst particles, relative to the more central parts, during the K-decay stage.

During the initial stages of K-decay, with only the catalyst in the bed (ToS > 32 h filled red squares in Figures 4–6), the catalytic activity is similar to the one attained during the last stages of K-saturation/equilibration (ToS ~30 to 32 h). The activity, as expressed in conversion terms, is at later stages diminished to a value that approximately corresponds to the initial catalytic activity for all of the compounds. This is consistent with the finding that at the end of the decay stage (ToS = 52 h), the catalyst very nearly had restored its initial sulfur coverage (see Figure 3).

The conversion achieved with the $MgAl_2O_4$ support during the decay stage (empty red squares in Figure 4–6 for ToS > 32 h) is considerably lower than the activity observed with the catalyst (filled red squares in Figures 4–6 for ToS > 32 h). However, in the case of naphthalene conversion (Figure 6), although it is lower than that for the $Ni/MgAl_2O_4$ catalyst, it is still significant for the K-doped $MgAl_2O_4$ carrier and approaches those of thermal effects only at the end of the K-decay stage. These results are consistent with earlier results, showing Na promotion of tar conversion over an alumina support.[60]

Table 4 presents the carbon formation on the $Ni/MgAl_2O_4$ and the support during the different experimental stages. As

Table 4. Specific Carbon Content on the Catalyst/Support (mg C/g_{cat})

experimental stage	$Ni/MgAl_2O_4$	$MgAl_2O_4$
aging	≤0.50	≤0.67
sulfidation	0.56	0.60
saturation stage	2.18	19.4
decay stage	0.67	35.7

seen, the carbon content on the $Ni/MgAl_2O_4$ catalyst increases from 0.56 to 2.2 mg/g_{cat} during the K-equilibration stage. This alternation may be the result of potassium–sulfur interactions on the nickel sites, allowing for carbon nucleation and growth on sulfur-free Ni sites. Despite this significantly increased but still very low C lay-down in the K-saturated stage compared to before K-dosing and after the K-decay stage, the activity of the catalyst is still greatly enhanced. The carbon lay-down in the K-saturation stage is comparable to the one reported by Moud et al.[35] (3.7 mg/g_{cat} after 36 h on stream), operating under similar conditions, using the same experimental setup and catalyst as in the present study.

The above result suggests that essentially carbon-free operation can be achieved with increased $Ni/MgAl_2O_4$ catalyst activity in the presence of a controlled amount of gas-phase potassium and high sulfur coverages on Ni. Nevertheless, during the decay stage, the carbon on the catalyst was found to decrease back almost to its original content of ≤0.5 mg/g_{cat}. For the $MgAl_2O_4$ support, the carbon deposits were measured to be as high as 19.43 mg/g_{cat} after the K-saturation period, and even higher (35.7 mg/g_{cat}) after the K-decay stage. The results demonstrate that the support alone is ineffective in gasifying the deposited carbon. Furthermore, given that K on the $MgAl_2O_4$ support gives rise to a significant naphthalene conversion, the deposited carbon on the support derives very likely primarily from the thermally rather unstable naphthalene and heavier tars. This can also explain why the amount of carbon deposited was lower on the $Ni/MgAl_2O_4$ catalyst after the K-decay stage compared to the K-saturated surface.

More carbon of a more reactive type on the catalyst in the absence of sulfur, compared to less carbon of a less reactive type on the catalyst in the presence of sulfur was observed by Xie et al.,[61] during steam reforming of liquid fuels at 800 °C. In their study, it was suggested that in the absence of S, quinone-like carbon structures are predominant on Ni,[61] which could readily decompose at high temperatures, facilitating carbon removal. In the presence of sulfur, graphitic carbon was expected to be deposited, which is more refractory and with less favorable gasification kinetics.[61] Therefore, the carbon surface coverage and reactivity could readily change with changes in S-coverage on Ni as we observe.

In Figure 7, the discussed interactions are summarized in a simplified scheme. Potassium effects are more pronounced for

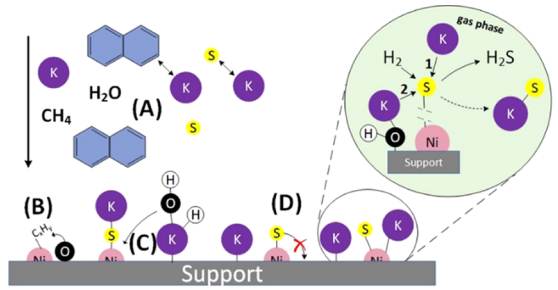

Figure 7. Simplified mechanisms of K–S interactions on $Ni/MgAl_2O_4$.

the heavier tar molecules in the gas phase (region A). Gas-phase potassium–sulfur interactions were not measured and thus cannot be excluded from the scheme. Region B in Figure 7 depicts the potentially more reactive (and oxygenated) carbon deposits on Ni at lower sulfur coverages when gas-phase K is present. Enhanced water splitting on K_{ads} and possible spillover of O(H) to Ni sites can also affect the S sorption and desorption rates, which in turn affect the catalyst activity (region C).

Region D indicates the preferential sorption of sulfur on the Ni sites. The K–S interaction due to surface diffusion of sulfur from Ni to the support is not probable. However, their interaction due to potassium surface diffusion from the support to the vicinity of the Ni sites is plausible (arrow 2 in inset). This interaction along with arrow 1, describing the interaction between gas-phase potassium with sulfur on the nickel sites, likely weakens the nickel–sulfur bond,[35] which in turn results in a lower S-coverage due to the equilibrium shifting toward gas-phase H_2S, as shown in Figure 7. The formation and desorption of the K–S complex from the support surface, as illustrated by the dashed line arrow, is based on our thermodynamic calculations not a likely thermodynamic sink for sulfur.

https://dx.doi.org/10.1021/acs.energyfuels.0c02069
Energy Fuels 2020, 34, 11103–11111

CONCLUSIONS

In the present work, the effects of gas-phase potassium on the activity of a sulfur-equilibrated $Ni/MgAl_2O_4$ catalyst was studied. Common aging, sulfidation, and potassium surface equilibration for both the catalyst and the support ($MgAl_2O_4$) were carried out to elucidate preferential adsorption of S and K species as well as to investigate the role of the support on the observed conversions.

Sulfur adsorbed only on the Ni sites of the $Ni/MgAl_2O_4$ proving the clear preferential adsorption of S on Ni sites, compared to the $MgAl_2O_4$ support. The K uptake was very similar on the $Ni/MgAl_2O_4$ catalyst and the pure $MgAl_2O_4$ support despite the high S content on the $Ni/MgAl_2O_4$ catalyst. It is therefore deemed that the preferential adsorption site for K is on the support but does not exclude a low but significant coverage of K on S−Ni sites or a higher coverage of K on a small fraction of Ni surface area, such as the Ni regions near the metal−support interface. It is also clear that K adsorption/desorption on/from the support readily takes place under steam reforming conditions. The K and S equilibration is fully reversible with θ_S on Ni, reestablishing the activity when K is being desorbed. Potential K−S interaction occurs most likely on the Ni sites or in the proximity of the Ni sites, while spillover of S from the Ni sites to the support is very small, if at all relevant.

The origin of the lower S-coverage on Ni upon K coadsorption during tar reforming conditions remains unsolved despite our additional studies here including also the $MgAl_2O_4$ carrier. We consider a plausible explanation for the reduction in S-coverage on Ni in the presence of gas-phase K to be related to high local concentrations of K and/or O(H) in the region near the metal−support interface, but further experiments are required to gain more detailed insight into the nature of species and their dynamics.

Introduction of K resulted in lower θ_S and a gradual, over time, drastic steam reforming activity increase for both light hydrocarbons and naphthalene, while at the same time slightly increasing the carbon deposition. Although the underlying mechanism for lowered θ_S on Ni when co-dosing gas-phase K remains unclear, e.g., related to faster oxygen transport from the support to Ni particles due to K-enhanced water splitting rates or just simply K-induced weakening of S−Ni bonds, we postulate simply that the increased population of S-free Ni sites results in higher probabilities to form larger ensembles of S-free Ni surface atoms better able to steam-reform larger and bulkier tar molecules. The reactivity of deposited carbon is high, which is supported by the established stable catalytic activity and the overall carbon deposition.

Importantly, we also find that the K-doped $MgAl_2O_4$ support contributed significantly to tar conversion, but not light hydrocarbon conversion.

The result suggests that an improved $Ni/MgAl_2O_4$ catalyst activity and an essentially carbon-free operation can be achieved in the presence of a controlled amount of gas-phase potassium and high sulfur coverages on Ni. Finally, simplified reaction mechanisms are proposed for the observed interactions.

AUTHOR INFORMATION

Corresponding Author

Klas Engvall − *Department of Chemical Engineering, KTH Royal Institute of Technology, SE-10044 Stockholm, Sweden;* orcid.org/0000-0002-6326-4084; Email: kengvall@kth.se

Authors

Asbel Hernandez − *Department of Chemical Engineering, KTH Royal Institute of Technology, SE-10044 Stockholm, Sweden; Department of Chemical Engineering, University of Rome Sapienza, 00184 Rome, Italy*

Klas J. Andersson − *Haldor Topsoe A/S, DK-2800 Kongens Lyngby, Denmark*

Efthymios Kantarelis − *Department of Chemical Engineering, KTH Royal Institute of Technology, SE-10044 Stockholm, Sweden*

Complete contact information is available at: https://pubs.acs.org/10.1021/acs.energyfuels.0c02069

Author Contributions

The manuscript was written through contributions of all authors. All authors have given approval to the final version of the manuscript.

Funding

This work was funded by the Swedish Center for Biomass Gasification (Svenskt Förgasningscentrum).

Notes

The authors declare no competing financial interest.

ACKNOWLEDGMENTS

The authors thank the Swedish Center for Biomass Gasification (Svenskt Förgasningscentrum) for funding this work and Haldor Topsoe A/S for providing the catalysts.

REFERENCES

(1) McKendry, P. Energy production from biomass (part 2): conversion technologies. *Bioresour. Technol.* **2002**, *83*, 47−54.

(2) Engvall, K.; Kusar, H.; Sjöström, K.; Pettersson, L. J. Upgrading of Raw Gas from Biomass and Waste Gasification: Challenges and Opportunities. *Top. Catal.* **2011**, *54*, 949−959.

(3) Devi, L.; Ptasinski, K. J.; Janssen, F. J. J. G. A review of the primary measures for tar elimination in biomass gasification processes. *Biomass Bioenergy* **2003**, *24*, 125−140.

(4) Kurkela, E.; Kurkela, M.; Hiltunen, I. Steam−oxygen gasification of forest residues and bark followed by hot gas filtration and catalytic reforming of tars: Results of an extended time test. *Fuel Process. Technol.* **2016**, *141*, 148−158.

(5) Milne, T. A.; Evans, R. J. *Biomass Gasifier "tars": Their Nature, Formation, and Conversion*, Report No. NREL/TP-570-25357; National Renewable Energy Laboratory (NREL): Golden, CO, 1998.

(6) Torres, W.; Pansare, S. S.; Goodwin, J. G. Hot Gas Removal of Tars, Ammonia, and Hydrogen Sulfide from Biomass Gasification Gas. *Catal. Rev.* **2007**, *49*, 407−456.

(7) Salo, K.; Mojtahedi, W. Fate of alkali and trace metals in biomass gasification. *Biomass Bioenergy* **1998**, *15*, 263−267.

(8) Turn, S.; Kinoshita, C. M.; Ishimura, D. M.; Zhou, J. The Fate of Inorganic Constituents of Biomass in Fluidized Bed Gasification. *Fuel* **1998**, *77*, 135−146.

(9) Nemanova, V.; Nordgreen, T.; Engvall, K.; Sjöström, K. Biomass gasification in an atmospheric fluidised bed: Tar reduction with experimental iron-based granules from Höganäs AB, Sweden. *Catal. Today* **2011**, *176*, 253−257.

(10) Dayton, D. *Review of the Literature on Catalytic Biomass Tar Destruction: Milestone Completion Report*; *Report* No. NREL/TP-510-

32815; National Renewable Energy Laboratory: Golden, CO (US), 2002.
(11) Chen, W.; Zhao, G.; Xue, Q.; Chen, L.; Lu, Y. High carbon-resistance Ni/CeAlO3-Al2O3 catalyst for CH4/CO2 reforming. *Appl. Catal., B* **2013**, *136*−*137*, 260−268.
(12) Yung, M. M.; Jablonski, W. S.; Magrini-Bair, K. A. Review of Catalytic Conditioning of Biomass-Derived Syngas. *Energy Fuels* **2009**, *23*, 1874−1887.
(13) Anis, S.; Zainal, Z. A. Tar reduction in biomass producer gas via mechanical, catalytic and thermal methods: A review. *Renewable Sustainable Energy Rev.* **2011**, *15*, 2355−2377.
(14) Sutton, D.; Kelleher, B.; Ross, J. R. H. Review of literature on catalysts for biomass gasification. *Fuel Process. Technol.* **2001**, *73*, 155−173.
(15) Wu, C.; Williams, P. T. Nickel-based catalysts for tar reduction in biomass gasification. *Biofuels* **2011**, *2*, 451−464.
(16) Cui, H.; Turn, S. Q.; Keffer, V.; Evans, D.; Tran, T.; Foley, M. Contaminant Estimates and Removal in Product Gas from Biomass Steam Gasification. *Energy Fuels* **2010**, *24*, 1222−1233.
(17) Fatehi, H.; He, Y.; Wang, Z.; Li, Z. S.; Bai, X. S.; Aldén, M.; Cen, K. F. LIBS measurements and numerical studies of potassium release during biomass gasification. *Proc. Combust. Inst.* **2015**, *35*, 2389−2396.
(18) Wellinger, M.; Biollaz, S.; Org Wochele, J.; Ludwig, C. Sampling and Online Analysis of Alkalis in Thermal Process Gases with a Novel Surface Ionization Detector. *Energy Fuels* **2011**, *25*, 4163−4171.
(19) Bridgwater, A. V. The technical and economic feasibility of biomass gasification for power generation. *Fuel* **1995**, *74*, 631−653.
(20) Mojtahedi, W.; Ylitalo, M.; Maunula, T.; Abbasian, J. Catalytic decomposition of ammonia in fuel gas produced in pilot-scale pressurized fluidized-bed gasifier. *Fuel Process. Technol.* **1995**, *45*, 221−236.
(21) Wangen, E. S.; Osatiashtiani, A.; Blekkan, E. A. Reforming of Syngas from Biomass Gasification: Deactivation by Tar and Potassium Species. *Top. Catal.* **2011**, *54*, 960−966.
(22) Rostrup-Nielsen, J.; Nielsen, P. *Progress in Catalyst Deactivation*, 1985; pp 259−323.
(23) Alstrup, I.; Clausen, B. S.; Olsen, C.; Smits, R. H. H.; Rostrup-Nielsen, J. R. Promotion of Steam Reforming Catalysts. In *Studies in Surface Science and Catalysis*; Elsevier, 1998; Vol. *119*, pp 5−14.
(24) Rostrup-Nielsen, J.; Christiansen, L. J. *Concepts in Syngas Manufacture*; Imperial College Press: London, 2011; Vol. *10*.
(25) Sehested, J.; Gelten, J. A. P.; Helveg, S. Sintering of nickel catalysts: Effects of time, atmosphere, temperature, nickel-carrier interactions, and dopants. *Appl. Catal., A* **2006**, *309*, 237−246.
(26) Shigehara, Y.; Ozaki, A. The effect of metallic potassium addition on catalytic properties of nickel for hydrogenation of ethylene. *J. Catal.* **1973**, *31*, 309−312.
(27) Bartholomew, C. H. Mechanisms of catalyst deactivation. *Appl. Catal., A* **2001**, *212*, 17−60.
(28) Bengaard, H. S.; Nørskov, J. K.; Sehested, J.; Clausen, B. S.; Nielsen, L. P.; Molenbroek, A. M.; Rostrup-Nielsen, J. R. Steam Reforming and Graphite Formation on Ni Catalysts. *J. Catal.* **2002**, *209*, 365−384.
(29) Einvall, J.; Albertazzi, S.; Hulteberg, C.; Malik, A.; Basile, F.; Larsson, A. C.; Brandin, J.; Sanati, M. Investigation of Reforming Catalyst Deactivation by Exposure to Fly Ash from Biomass Gasification in Laboratory Scale. *Energy Fuels* **2007**, *21*, 2481−2488.
(30) Albertazzi, S.; Basile, F.; Brandin, J.; Einvall, J.; Fornasari, G.; Hulteberg, C.; Sanati, M.; Trifirò, F.; Vaccari, A. Effect of fly ash and H2S on a Ni-based catalyst for the upgrading of a biomass-generated gas. *Biomass Bioenergy* **2008**, *32*, 345−353.
(31) Wangen, E. S.; Osatiashtiani, A.; Blekkan, E. A. Reforming of Syngas from Biomass Gasification: Deactivation by Tar and Potassium Species. *Top. Catal.* **2011**, *54*, 960−966.
(32) Jiang, X.; Li, C.; Chi, Y.; Yan, J. TG-FTIR study on urea-formaldehyde resin residue during pyrolysis and combustion. *J. Hazard. Mater.* **2010**, *173*, 205−210.
(33) Li, Y. P.; Wang, T. J.; Wu, C. Z.; Gao, Y.; Zhang, X. H.; Wang, C. G.; Ding, M. Y.; Ma, L. L. Effect of Alkali Vapor Exposure on Ni-MgO/γ-Al2O3/Cordierite Monolithic Catalyst for Biomass Fuel Gas Reforming. *Ind. Eng. Chem. Res.* **2010**, *49*, 3176−3183.
(34) Moud, P. H.; Andersson, K. J.; Lanza, R.; Pettersson, J. B. C.; Engvall, K. Effect of gas phase alkali species on tar reforming catalyst performance: Initial characterization and method development. *Fuel* **2015**, *154*, 95−106.
(35) Moud, P. H.; Andersson, K. J.; Lanza, R.; Engvall, K. Equilibrium potassium coverage and its effect on a Ni tar reforming catalyst in alkali- and sulfur-laden biomass gasification gases. *Appl. Catal., B* **2016**, *190*, 137−146.
(36) Rostrup Nielsen, J. R. Some principles relating to the regeneration of sulfur-poisoned nickel catalyst. *J. Catal.* **1971**, *21*, 171.
(37) Alstrup, I.; Rostrup-Nielsen, J. R.; Røen, S. High temperature hydrogen sulfide chemisorption on nickel catalysts. *Appl. Catal.* **1981**, *1*, 303−314.
(38) Elliott, D. C.; Baker, E. G. The effect of catalysis on wood-gasification tar composition. *Biomass* **1986**, *9*, 195−203.
(39) Brage, C.; Yu, Q.; Chen, G.; Sjöström, K. Use of amino phase adsorbent for biomass tar sampling and separation. *Fuel* **1997**, *76*, 137−142.
(40) Dybkjaer, I. Tubular reforming and autothermal reforming of natural gas — an overview of available processes. *Fuel Process. Technol.* **1995**, *42*, 85−107.
(41) Pala, L. P. R.; Wang, Q.; Kolb, G.; Hessel, V. Steam gasification of biomass with subsequent syngas adjustment using shift reaction for syngas production: An Aspen Plus model. *Renewable Energy* **2017**, *101*, 484−492.
(42) Veksha, A.; Giannis, A.; Da Oh, W.; Chang, V. W.-C.; Lisak, G.; Lim, T. T. Catalytic activities and resistance to HCl poisoning of Ni-based catalysts during steam reforming of naphthalene. *Appl. Catal., A* **2018**, *557*, 25−38.
(43) Praliaud, H.; Primet, M.; Martin, G. A. Physico-chemical properties of potassium-promoted Ni/SiO2 catalysts. *Appl. Surf. Sci.* **1983**, *17*, 107−123.
(44) Papageorgopoulos, A. C.; Kamaratos, M. K and S coadsorption on Ni(100) surfaces. *J. Phys.: Condens. Matter* **2000**, *12*, 9281−9291.
(45) Li, M. R.; Lu, Z.; Wang, G. C. The effect of potassium on steam-methane reforming on the Ni4/Al2O3 surface: a DFT study. *Catal. Sci. Technol.* **2017**, *7*, 3613−3625.
(46) Bornemann, T.; Steinrück, H. P.; Huber, W.; Eberle, K.; Glanz, M.; Menzel, D. The adsorption of H2O on K precovered Ni(111) studied by ARUPS and TPD. *Surf. Sci.* **1991**, *254*, 105−118.
(47) Kotarba, A.; Dmytrzyk, J.; Narkiewicz, U.; Baranski, A. Sulfur Poisoning of Iron Ammonia Catalyst Probed by Potassium Desorption. *React. Kinet. Catal. Lett.* **2001**, *74*, 143−149.
(48) Błaszczyszyn, R.; Błaszczyszynowa, M.; Gubernator, W. Thermal Desorption of Potassium from Clean and Sulfur Covered Nickel. *Acta Phys. Pol., A* **1995**, *88*, 1151−1160.
(49) Borowiecki, T.; Denis, A.; Rawski, M.; Gołębiowski, A.; Stołecki, K.; Dmytrzyk, J.; Kotarba, A. Studies of potassium-promoted nickel catalysts for methane steam reforming: Effect of surface potassium location. *Appl. Surf. Sci.* **2014**, *300*, 191−200.
(50) Hamlyn, R. C. E.; Mahapatra, M.; Orozco, I.; Waluyo, I.; Hunt, A.; Rodriguez, J. A.; White, M. G.; Senanayake, S. D. Structure and Chemical State of Cesium on Well-Defined Cu(111) and Cu2O/Cu(111) Surfaces. *J. Phys. Chem. C* **2020**, *124*, 3107−3121.
(51) Gai, C.; Dong, Y.; Yang, S.; Zhang, Z.; Liang, J.; Li, J. Thermal decomposition kinetics of light polycyclic aromatic hydrocarbons as surrogate biomass tar. *RSC Adv.* **2016**, *6*, 83154−83162.
(52) Bach-Oller, A.; Furusjö, E.; Umeki, K. On the role of potassium as a tar and soot inhibitor in biomass gasification. *Appl. Energy* **2019**, *254*, No. 113488.
(53) Bartholomew, C. H.; Agrawal, P. K.; Katzer, J. R. Sulfur Poisoning of Metals. In *Advances in Catalysis*; 1982; Vol. *31*, pp 135−242.
(54) Bailey, K. M.; Campbell, T. K.; Falconer, J. L. Potassium promotion of Ni/Al2O3 catalysts. *Appl. Catal.* **1989**, *54*, 159−175.

https://dx.doi.org/10.1021/acs.energyfuels.0c02069
Energy Fuels 2020, 34, 11103−11111

(55) Horvat, A.; Kwapinska, M.; Xue, G.; Dooley, S.; Kwapinski, W.; Leahy, J. J. Detailed Measurement Uncertainty Analysis of Solid-Phase Adsorption—Total Gas Chromatography (GC)-Detectable Tar from Biomass Gasification. *Energy Fuels* **2016**, *30*, 2187−2197.
(56) Froment, G. B.; DeWilde, J.; Bischoff, K. B. *Chemical Reactor Analysis and Design*, 3rd ed.; Wiley, 2011.
(57) Xu, J.; Froment, G. F. Methane steam reforming: II. Diffusional limitations and reactor simulation. *AIChE J.* **1989**, *35*, 97−103.
(58) Da Cruz, F. E.; Karagöz, S.; Manousiouthakis, V. I. Parametric Studies of Steam Methane Reforming Using a Multiscale Reactor Model. *Ind. Eng. Chem. Res.* **2017**, *56*, 14123−14139.
(59) Bird, R. B.; Stewart, W. E.; Lightfoot, E. N. *Transport Phenomena*, 2nd revised ed.; John Wiley & Sons: New York, 2007.
(60) Mudge, L. K.; Baker, E. G.; Mitchell, D. H.; Brown, M. D.; Sol, J. Catalytic Steam Gasification of Biomass for Methanol and Methane Production. *J. Sol. Energy Eng.* **1985**, *107*, 88−92.
(61) Xie, C.; Chen, Y.; Li, Y.; Wang, X.; Song, C. Influence of sulfur on the carbon deposition in steam reforming of liquid hydrocarbons over CeO2−Al2O3 supported Ni and Rh catalysts. *Appl. Catal., A* **2011**, *394*, 32−40.

https://dx.doi.org/10.1021/acs.energyfuels.0c02069
Energy Fuels 2020, 34, 11103−11111